INTERNATIONAL SOCIETY FOR SOIL MECHANICS AND GEOTECHNICAL ENGINEERING

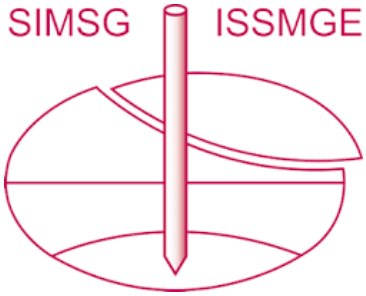

This paper was downloaded from the Online Library of the International Society for Soil Mechanics and Geotechnical Engineering (ISSMGE). The library is available here:

https://www.issmge.org/publications/online-library

This is an open-access database that archives thousands of papers published under the Auspices of the ISSMGE and maintained by the Innovation and Development Committee of ISSMGE.

The paper was published in the proceedings of the 17th African Regional Conference on Soil Mechanics and Geotechnical Engineering and was edited by Prof. Sw Jacobsz. The conference was held in Cape Town, South Africa, on October 07-09 2019.

The mineralogical composition and shear behaviour of loess-like deposits in Mount Moorosi Village in Lesotho

M. Damane, D. Kalumba & L. Sobhee-Beetul
University of Cape Town, Cape Town, South Africa

ABSTRACT: Most structures constructed in Mount Moorosi have sustained severe cracks and the potential cause could be the underlying loess like deposits which are renowned for inducing the saturated strength problems. Therefore, the shear stress-strain behaviour of this soil was herein experimentally investigated in specimens at saturated and natural moisture contents. The evaluation was achieved by performing a series of consolidated undrained triaxial tests. Additionally, the mineralogical composition, which substantially affects the properties in loess, was quantified from the x-ray diffraction. The stress-strain analysis demonstrated a relatively high shear strength parameters at field moisture, and a drastic reduction in saturated specimens which clearly showed soil strength moisture dependency. The XRD results showed that the tested samples predominantly consisted of the passive minerals (quartz, feldspar and mica) with more than 10 % of the active minerals (kaolinite, carbonates, halide, oxides and hydroxides). The mineralogy quantification further revealed that the cohesive fabric was primarily rendered by kaolinite. The findings of this study could be adopted in foundation designs, rehabilitation and research in potential ground improvement techniques.

1 INTRODUCTION

1.1 *Background*

Loessal soil is the most prevalent collapsible soil covering a mean of 10 % of the land area of the world (Howayek et al. 2012). Its global geographical distribution was highlighted in Asia, Europe, Australia and the United States of America (Pye 1987). It has also been identified in North Africa and Namibia (Assallay et al. 1996, Nouaouria et al. 2008, Crouvi et al. 2010).

The passive minerals in loess include quartz (20 to 85 %), feldspar (4 to 40 %) and mica (1 to 30 %), while the remaining active minerals consist of calcite (0.2 to 30 %), gypsum (0.0 to 3 %), salt (0.0 to 2 %) and clays (Egri 1972). The passive particles predominantly comprise silt making 50 to 70 % by weight (Nouaouria et al. 2008), and are bonded by the active aggregations to form a high shear strength cohesive fabric at relatively low moisture content. Conversely, the documented cases on saturation of these deposits have shown loss of shear strength and volume change that trigger catastrophic landslides, sinkholes and building settlement (Berg 1964, Grigoryan 1991, Djogo & Milović 2013, Yuan-xun et al. 2013, Peng 2015). The dissolution of the wetted cementing grains and reduced shear strength induces hydrocollapse settlement and bearing capacity problems on the superimposed civil engineering structures. Therefore, understanding the variation in shear behaviour of lightly wetted and saturated soils is important for durable construction.

Most houses in the Mount Moorosi village have sustained severe stair-stepped and shear cracks which could be related to the possible underlying loess-like soil movements (Damane 2019). Therefore, this study was primarily aimed at experimentally investigating the shear behaviour of these deposits at the saturated and natural moisture conditions. Several Consolidated Undrained (CU) shear tests were conducted on GEOCOMP triaxial equipment. Moreover, it was imperative to quantify the mineralogical composition by X-Ray Diffraction (XRD) analysis; the minerals mainly affect the soil shear and volume change properties (Liu et al. 2015). The findings of this research were expected to show the mineralogical composition and shear strength moisture dependency which could be useful in foundation designs.

1.2 *Study area and geological setting*

Mount Moorosi village is located 39.8 km north-east of Moyeni in the Quthing district of southern Lesotho. It is situated at an average latitude of 30°16'39.76" S and longitude of 27°52'14.98" E within the Senqu valley agroecological zone at a mean elevation of 1700 m above mean sea level. It is positioned at the base of Mokotjomela Mountain in the Clarens and upper Elliot sub-lands of the Stormberg formation in the Karoo basin. Three diverse types of sedimentary

rocks which include sandstones, siltstones and mudstones have been reported in these landforms (Brink 1983, Rooy & Schalkwyk 1993). Highly erodible loess like deposits of over 3 m in thickness were also identified (Damane, 2019). Figure 1 depicts the studied region of the Mount Moorosi village.

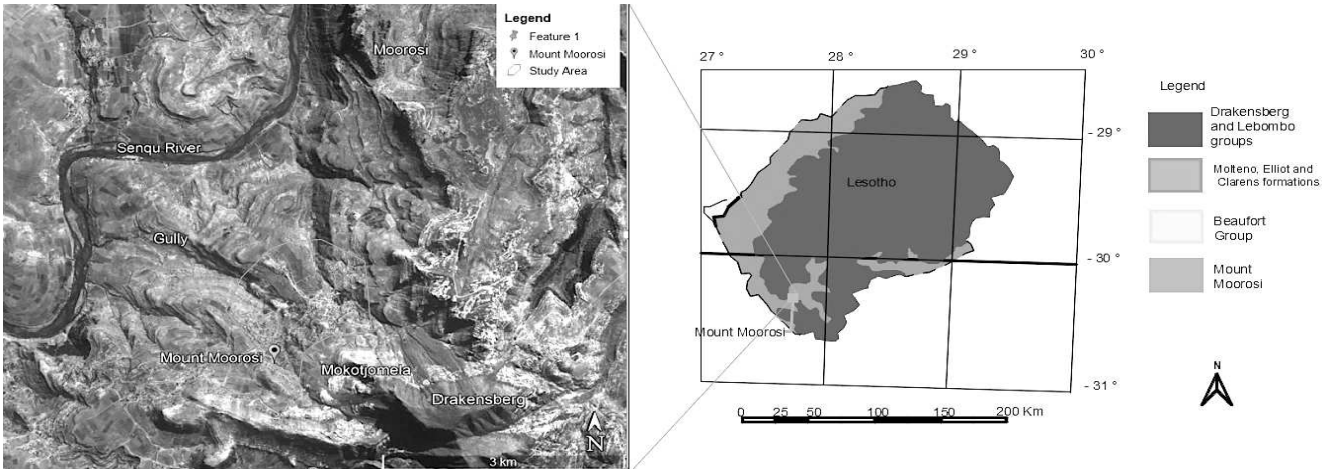

Figure 1. Study area (modified from the Republic of South Africa mineral map, 2018)

2 EXPERIMENTATION

2.1 *Materials*

The representative soil samples were excavated from three different sites in the Mount Moorosi residential settlement and transported to the geotechnical laboratory at the University of Cape Town (UCT) for analysis. Index tests were performed according to the British Standard procedures (BS 1377-2-1990), specifically for soil classification. In-situ density and moisture were also determined using a Troxler for the preparation of the reconstituted CU specimens. Based on Table 1, the tested samples had low plasticity with clay content ranging from 8 to 12 %. The silt particles were the most abundant with a maximum value of 78 %, followed by sand which ranged from 12 to 23 %. This grain size distribution is comparable to that of Libyan loess reported by Assallay et al. (1996). However, the high densities are similar to those published by Anagnostic (1973) and Klukanova & Frankovska (1995) in Libya and Slovakia, respectively.

Table 1. Summary of index properties of Mount Moorosi soil

Sample property	Sample location		
	Site 1	Site 2	Site 3
Specific gravity (g/cm^3)	2.60	2.65	2.59
Field moisture content (%)	8.2	7.6	6.8
Field bulk density (kg/m^3)	1818	2021	1958
Relative compaction (%)	85	92	87
Particle size distribution			
Clay (%)	9.7	8.0	12.0
Silt (%)	66.3	78.0	70.0
Sand (%)	23.0	12.0	18.0
Atterberg limits			
Liquid limit (%)	33.0	28.7	26.0
Plastic limit (%)	16.0	14.7	14.0
Plasticity index (%)	17.0	14.0	12.0
Linear Shrinkage (%)	5.04	5.80	5.66
USCS*	CL	CL	CL

* USCS = Unified Soil Classification System.

Approximately 70 % of the particles passed the 0.063 mm sieve during wet sieving, hence the XRD analysis was executed on fine grains (< 0.063 mm). For CU testing, the samples passing the 5 mm sieve were used based on BS 1377-4-1990 recommendations.

2.2 *Experimental procedure*

2.2.1 *X-ray diffraction*

The mineralogy quantification was performed at the Centre for Minerals Research based at UCT, and the procedure proposed by Coelho (2007) was followed. This involved micronising the prepared representatives in ethanol using a McCrone micro-niser for homogeneous grain size distribution. Then the powder XRD spectra were attained by means of Bruker D8 advance powder diffractometer with Vantec detector and fixed divergence. The resulting slits were received with Co-Ka radiation. For phase identification, Bruker Topas 4.1 software (Coelho 2007) was used and their corresponding amounts (weight %) were estimated using the Rietveld method.

2.2.2 *Consolidated undrained shear test*

The consolidated undrained shear strength investigation was done for a series of confining pressures (50, 100 and 250 kPa) for each set of field moistures and densities. The various stresses were selected to evaluate the field shear behaviour under diverse possible loadings, and to determine the corresponding shear strength parameters. The tests were performed on saturated as well as samples at field moisture content on a calibrated GEOCOMP triaxial apparatus. The saturated conditions presented an important opportunity to simulate the change in field shear strength during the rainy period. These tests circumstances were relevant to the study area since the lands are exposed to

annual surplus rainfall in summer and cold dry environment in winter.

For quality assurance, the preparation of the specimens was in accordance with British Standard test methods (BS 1377-4-1990). The tests were conducted on soil which was thoroughly mixed with the required water and left for a maturing period of 24 hours in an airtight plastic bag. Table 2 presents the number of layers and drops that were required to compact the soil for the various test sets. The height of the specimens was approximately 104 mm and the respective diameter was 52 mm. These dimensions were recommended by BS 1377-4-1990 to achieve the accurate shearing.

Table 2. Triaxial tests Compaction summary (Damane 2019)

Site	C*	P*	M*	L*	D*
1	Natural	250	7.8	6	25
		100	7.8	6	25
		50	7.7	6	25
	Wet	250	16.1	6	25
		100	15.5	6	25
		50	15.5	6	25
2	Natural	250	7.4	6	38
		100	7.4	6	38
		50	7.4	6	38
	Wet	250	12.5	6	38
		100	13.2	6	38
		50	11.5	6	38
3	Natural	250	6.4	6	35
		100	6.5	6	35
		50	6.4	6	35
	Wet	250	12.4	6	35
		100	12.9	6	35
		50	13.4	6	35

* C = Moisture state, * P = Confining pressure, * M = Moisture content, * L = Number of layers, * D = Number of drops.

A 2.5 kg rammer used in compacting soil layers was falling at a height of 200 mm. This compaction was done in a split mould, and it should be noted that many trials which involved varying the height of fall, number of blows and layers were done to achieve the target field density.

The compacted specimen was transferred to a base pedestal of the Triaxial cell where it was gently encapsulated by a 0.2 mm thick latex membrane using a stretcher mould. The rubber o-rings were also equally fitted on the bottom and top caps, and the loading piston was clamped on the cell body which was finally filled with tap water. The triaxial cell was then centrally positioned on a GEOCOMP loadtrack and the piston was brought in contact with the load frame. The two flow tracks were then connected to the pedestal.

For the final test set-up, the American testing method (ASTM D4767-11) was used. The first phase in a saturated CU test set-up involved wetting the specimen to a saturation ratio of 0.9 and duration of 24 hours based on the findings of Black & Lee (1973). This phase was followed by the consolidation in which a stress was applied at a rate of 13.7895 kPa/min to a maximum time of 12 hours and a minimum of 1 hour. The final stage was shear at a rate of 0.02 mm/min to a maximum strain of 22 %. The same setting-up was followed for all the samples with the only changes in the confining pressures. In addition, the saturation phase was set to zero for the specimens tested at in-situ moisture content. Figure 2 depicts an assembled apparatus for triaxial test and a compacted specimen on a pedestal.

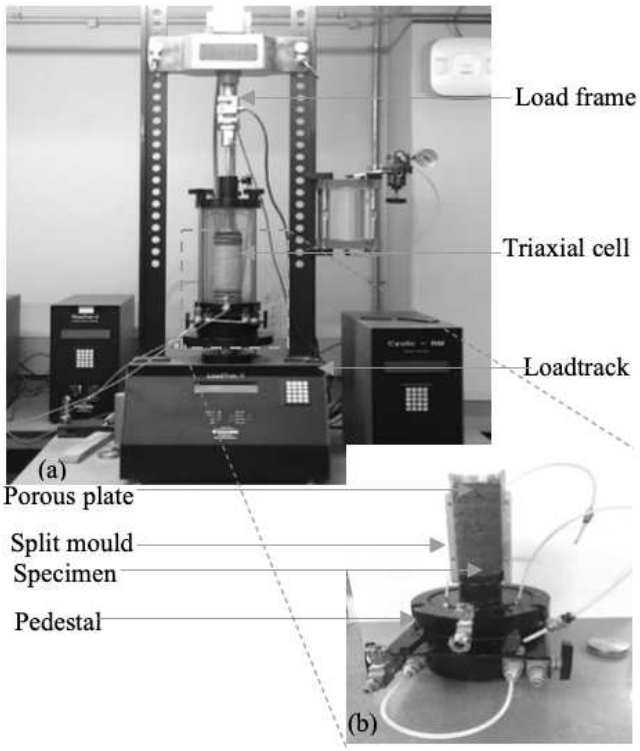

Figure 1. Apparatus for triaxial test, (a) assembled apparatus for triaxial testing and (b) compacted specimen on a pedestal.

3 RESULTS AND ANALYSIS

3.1 *X-ray diffraction*

Figure 3 presents the graphical plots obtained from XRD tests. The analysis of the intensities plotted against 2theta facilitated in the quantification of the minerals existing in the representative samples. To detect the diffraction of rays by atomic planes in any possible orientation, a 2theta (i.e. diffraction angle) ranging from 10 to 120° was selected. The highest intensity was recorded at 2theta between 25 and 35°. Clearly, this range corresponded to the orientation of most of the atomic planes and the spectrum demonstrated small intensities beyond it. The intensities represented quartz, albite feldspar, anorthite feldspar, mica, kaolinite, halide, sulfate, carbonates, sulfate, halide, the oxides and hydroxides of iron and aluminum. All the graphs from the different sites retained a comparable pattern demonstrating insignificant dissimilarity in mineralogical composition of the soil from the various sites.

Table 3. Mineral summary of loess like soil in Mount Moorosi

Sample	Q*	Feldspar			B*	Gb*	Ka*	Carbonates			Gy*	Go*	Ha*
Location		Al*	An*	Total				Ca*	Do*	Total			
Site 1	40.04	14.00	19.04	33.04	11.09	2.60	7.75	0.83	0.26	1.09	0.62	0.08	0.67
Site 2	45.70	11.33	19.74	31.06	11.02	2.12	7.21	1.42	0.06	1.47	0.61	0.26	0.57
Site 3	40.81	14.03	17.13	31.15	13.74	3.05	9.13	0.58	0.16	0.73	0.65	0.15	0.63

* Q = Quartz, * Al = Albite, * An = Anorthite, * B = Biotite 1M mica, * Gb = Gibbsite (aluminium oxides and hydroxides), * Ka = Kaolinite (clay), * Ca = Calcite (carbonate), * Do = Dolomite (carbonate),* Gy = Gypsum (Sulfate), * Go = Goethite (iron oxides and hydroxides), * Ha = Halite (Halide) (salt)

.

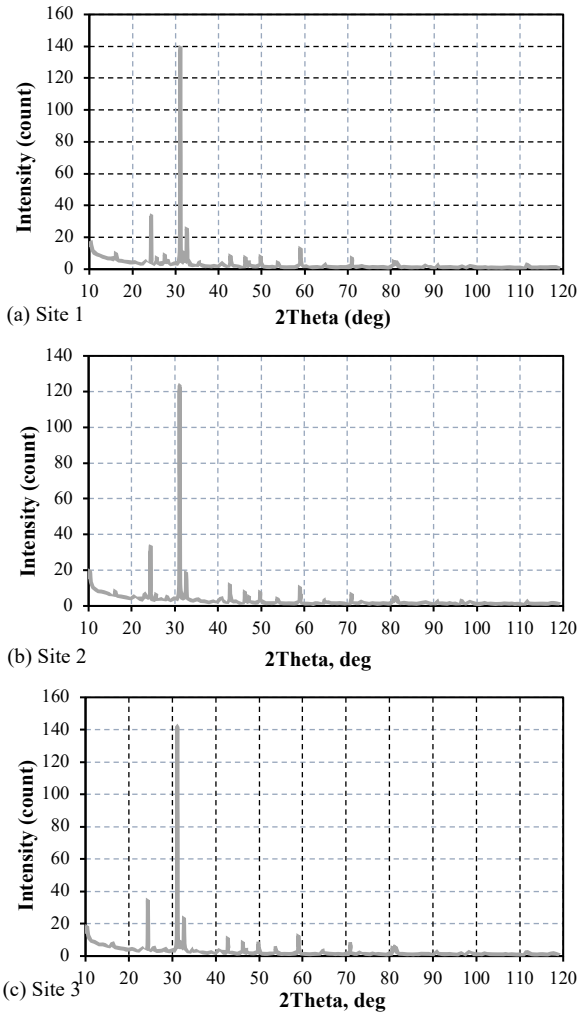

Figure 2. XRD intensities against 2Theta (Damane 2019)

Table 3 shows the quantification of the identified minerals. It was noted that quartz was the most prevalent with an average of 42 % and was followed by feldspar (32 %). Mica was the third-most abundant with a mean value of 12 %. Although illite is common in loess, kaolinite was the only clay and primary cementing mineral detected in the analysed samples ($\approx$ 8 %). This could be attributed to the mineralogical composition of the parent rock or the fact that clay minerals are formed under the different environments (Grim 1953). Gebbsite, also one of the building blocks in clays, had a mean value of 3 %. In fact, investigations have shown that it is precipitated from the dissolution of the primary kaolinite in highly weathered or leached soils (Muggler et al. 2007, Marcelino et al. 2010). It is evident from this observation that kaolinite in assessed soil becomes active on saturation and can perhaps contribute to change in properties like shear strength and the subsequent hydrocollapse. Other crystals, also soluble in water, made an average of 3 % (calcite, dolomite, gypsum, goethite and halite). This shows that more than 10 % of the minerals in these deposits possibly become active when the soil is wetted, hence triggering the mobility of the core grains and reducing the soil shear strength.

3.2 *Consolidated undrained shear strength*

3.2.1 *Deviator stress-strain relationship: at natural moisture content*

Figures 4 a, b, c, d, e and f present the deviator/shear stress-strain graphical plots for various confining pressures (50, 100 and 250 kPa) in specimens from all the three sites. Figures 4 a, c and e were plotted based on the tests sheared at in-situ moisture content. Generally, the shear stress $(\sigma_1 - \sigma_3)$ increased quickly with minor augmentation in the strain until a yielding stress was reached. Beyond the peak point, the shear stress gradually reduced as the strain was increased until the test was ended. In all the graphs, the maximum peak occurred at the highest confining stresses, whereas the least values were produced in lower pressure. This was ascribed to the high grain confinement at large initial pressure which enhanced the interparticle contact area, thus the shear resistance.

The yielding points were well defined and rapidly reached at a strain of nearly 2 % at a confining pressure of 50 kPa. Such peaks were attributed to the interlocking and interparticle frictional resistance which had to be overcome for shear mobilisation to occur. Therefore, the soil grains moved up and over the neighbouring ones (dilation) and the stress that resisted this dilation was manifested in the form of the peak deviator stress. Once the interlocking was reduced, the grains were easily sheared, and this resulted in decreased deviator stress with rise in strain.

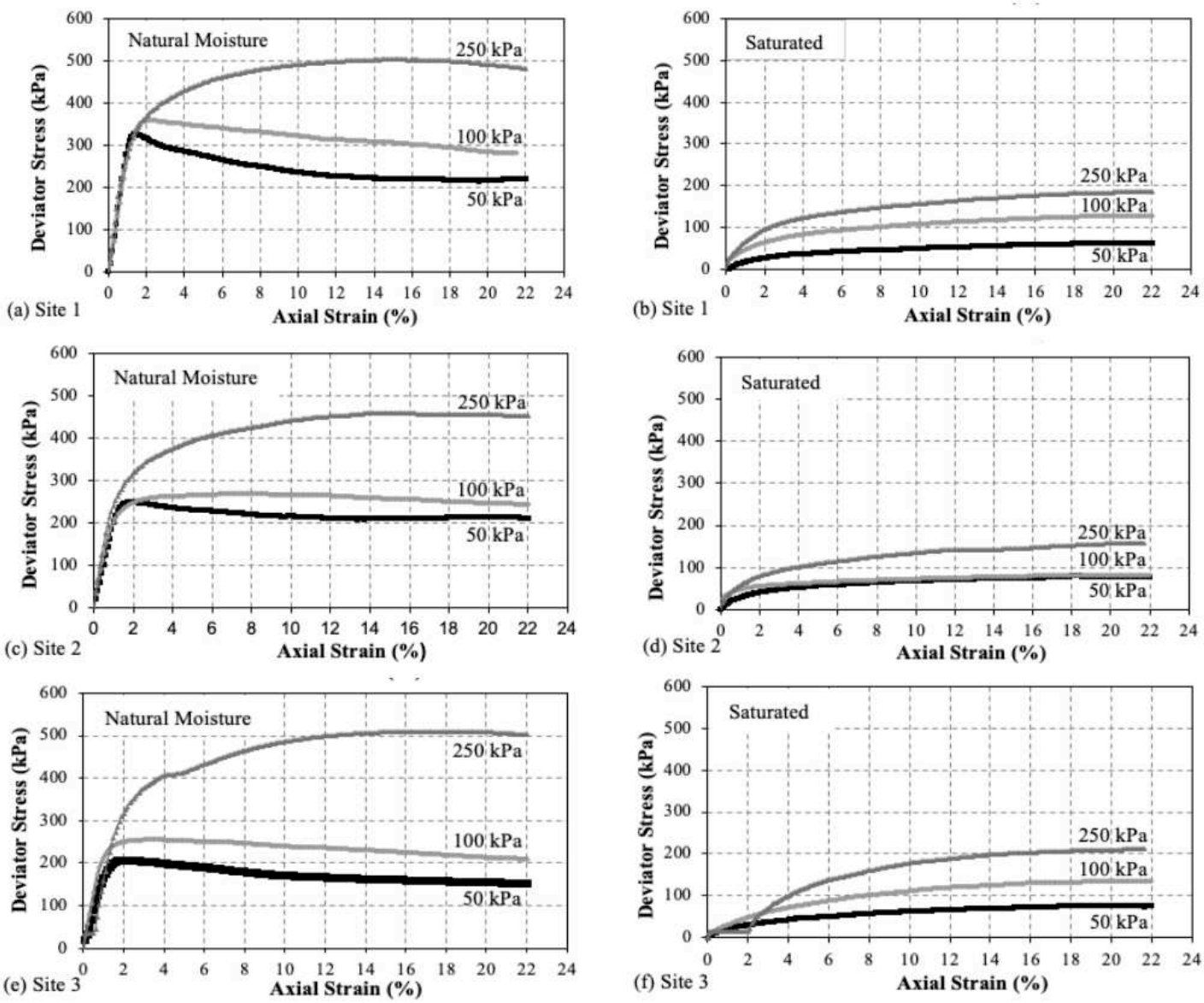

Figure 4. Consolidated undrained triaxial plot of deviator stress against axial strain (Damane 2019)

A deviator stress-strain plot similar to that of a confining stress of 50 kPa, was produced by a pressure of 100 kPa, but at a slightly greater strain (< 4 %) due to higher confinement. However, the yielding points were not as well distinct. This showed the partial resistance of the particles to dilation. A rather smooth curve was produced at a stress of 250 kPa with higher maximum deviator stress. This was indicative that the confining pressure was beyond the yield stress which prevented the particles from dilating. The shear strength in such curves was ascribed to the particles crushing resistance (Bolton 1986).

3.2.2 *Deviator stress-strain relationship: at saturated moisture content*

Figures 4b, d and f illustrate the smooth graphical plots for the saturated tests with the comparable failure trend, and no distinct peaks. The interparticle space that was augmented by the development of the pore water pressure during the consolidation phase, was associated with the observed smooth curves. The pore pressure was approximately 2 kPa in all the samples tested at field moisture, while higher values (over 40, 90 and 240 kPa in confining pressures of 50, 100 and 250 kPa respectively) occurred in saturated tests. The enlarged spaces between the particles subsequently reduced the friction resistance which increased the particles mobility during shearing, hence the low deviator stress with smooth curves. Further increase in straining gradually reduced these spaces and improved the contact area which in turn slowly enhanced the shear stress.

3.2.3 *Shear Strength Parameters*

Table 4 presents the shear strength parameters (i.e. cohesion and friction angle) determined from all the tests. Generally, they were relatively high at natural water quantity and drastically reduced at saturated conditions. This was possibly caused by the attraction such as the Van der Waal forces which depend on spaces between the individual particles (Adair & Sindel et al. 2001). Cohesive attraction in loess

increases with the amount of water until a specific threshold is reached beyond which it reduces (Langfelder & Nivargikar 1967). The reduction is due to the grain dispersion by the pore water.

Table 4. Measured shear strength parameters in soils in Mount Moorosi

Sample	Moisture	Shear strength parameters	
Location	Condition	Cohesion (kPa)	Friction angle (°)
Site 1	Natural	100	18
	Wet	20	13
Site 2	Natural	61	21
	Wet	21	10
Site 3	Natural	36	26
	Wet	21	14

The cohesion in samples from the various sites was significantly different in tests conducted at in-situ moisture due to the variation in the initial water content (refer to Table 1). The highest cohesion (100 kPa) was demonstrated by samples from site 1 with a moisture content of 7.8 % and the similar specimens had the least value (20 kPa) at a mean water quantity of 15.5 %. The friction angle was also decreased in saturated tests because of the pore pressure which weakened the frictional resistance.

4 CONCLUSION

From the investigation on the mineralogical composition and shear behaviour of the loess like deposit in the Mount Moorosi village, it was concluded that: Quartz (42 %) was the most prevalent passive mineral followed by feldspar (32 %) and then mica (12 %). Kaolinite, a primary cementing mineral in the studied samples, made up approximately 8 % by composition and was precipitating to gibbsite (3 %). Other active and soluble minerals reached an average of 3 % by composition. Therefore, more than 10 % of the minerals possibly became active on saturation.

At low confining pressure (50 kPa) in tests at field moisture, the soil was dilative and formed peak stresses at strains less than 2 %. The soil particles became less dilative at higher confining pressures which resulted in less distinct peaks and smooth curves at 100 and 250 kPa, respectively. In saturated circumstances, a drastic reduction in shear stress occurred and the curves remained smooth due to enlarged interparticle spaces by the pore water pressure. Water reduced cohesion by a highest value of 80 %, while friction angle was by 46 %.

5 ACKNOWLEDGMENTS

The authors are grateful to MasterCard Foundation Programme at the University of Cape Town for funding this research. Mr. Elvino Witbooi, a Technician at the university geotechnical laboratory is also appreciated for his invaluable assistance.

6 REFERENCES

Adaira, J.H. Suvacib, E. & Sindela, J. 2001. Surface and Colloid Chemistry: *Encyclopedia of Materials: Science and Technology, Second Edition:*1-10.

Arvind, R. 2016. Investigation of cracks in buildings. *ResearchGate.*

Assallay, A.M. Rogers, C.D.F. & Smalley, I.J. 1996. Engineering properties of loess in Libya. *Journal of Arid Environments.* 32: 373-386.

American Standard Test Methods (ASTM D4767-11). Standard test method for consolidated undrained triaxial compression test for cohesive soils.

Berg, L.S. 1964. Loess as a product of weathering and soil formation. Israel Program for Science Translations. 207.

Black, D.K & Lee, K. 1973. Saturating laboratory samples by back pressure: *Journal of soil mechanics and foundations.* 99: 75-93.

Bolton, M.D. 1986. The strength and dilatancy of sands: *Geotechnique*. 36(I): 65-78.

Brink, A.B.A. 1983. *Engineering geology of southern Africa Volume 3*. Cape Town: Building publications.

British Standard (BS 1377-2-1990). Methods of test for Soils for civil engineering purposes, Part 2: Classification tests.

British Standard (BS 1377-4-1990). Methods of test for Soils for civil engineering purposes, Part 4: Compaction-related tests.

Coelho, A. 2007. TOPAS-Academic, Coelho Software, Brisbane, Australia.

Crouvi, O. Amit, R. Enzel Y. & Gillespie R.A. 2010. Active sand seas and the formation of desert loess. *Quaternary Science Reviews.* 29: 2087-2098.

Damane, M. 2019. An investigation into the volume change characteristics of loess like deposits in Mount Moorosi, Lesotho. Master's dissertation: University of Cape Town.

Djogo, M. & Milović, D. 2013. Differential settlement of foundations on loess. In *Seventh international conference on case histories in geotechnical engineering. Missouri University of Science and Technology.*

Egri, G. 1972. The physico-chemical properties and engineering problems of the loess soils: *Acta Gelo. Acad, Sci. Hung.* 16: 337-345.

Grigoryan. A.A. 1991. Construction on loess soil.

Grim, R.E. 1953. *Clay Mineralogy*. New York, Toronto, London: McGraw-Hill Book Company, INC.

Howayek, A.E.I. Huang, P. Bisnett, R. & Santagata, M.C. 2011. Identification and behavior of collapsible soils: *Joint transportation research program*, FHWA/IN/JTRP-2011/12.

Klukanova, A. & Frankovska, J. 1995. The slovak carpathians loess sediments, their fabric and properties.Genesis and properties of collapsible soils. London and New York, Plenum Publishing Corporation.

Liu, Z. Liu, F. Ma, F. Wang, M. Bai, X. Zheng, Y. Yin, H. & Zhang, G. 2015. Collapsibility, composition, and microstructure of a loess in China. *Canadian Geotechnical Journal.*

Nouaouria, M.S. Guenfoud, M. & Lafifi, B. 2008. *Engineering properties of loess in Algeria. Engineering Geology.* 99: 85-90.

Marcelino, V. Stoops, G. & Schaefer, C.E.G.R. 2010. Interpretation of micromorphological features of soils and regoliths. 14-Oxic and related materials. *Elsvier*: 305-327.

Muggler, C.C. Buurman, P. & Doesburg, V.J.D.J. 2007. Weathering trends and parent material characteristics of polygenetic oxisols from Minas Gerais, Brazil: Mineralogy. *Geoderma*. 138: 39-48.

Peng, J. Fana, Z. DiWua, Zhuang, J. Dai, F. Chenc, W. & Zhao, C. 2015. Heavy rainfall triggered loess-mudstone landslide and subsequent debris flow in Tianshui: *China: Engineering geology.* 186: 79-90.

Pye, K. 1987. *Aeolian dust and dust deposits*. London: Academic press.

Rooy, J.L.V & Schalkwyk, A.V. 1993. The geology of the Lesotho Highlands Water Project with special reference to the durability of construction materials: *Journal of African Earth Sciences.* 16(1/2): 181-192.

Rowell, D.L. 2014. *Soil science: Methods and applications*. New York, Routledge.

Whitlow, R. 1995. *Basic of soil mechanics: Third edition*. England: Longman group limited.

Yuan-xun, L. Yan-peng, Z. Shuai-hua, Y. & Zhong-mao, H. 2013. Analysis of foundation non-uniform settlement for building on collapsible loess. *Applied Mechanics and Materials.* 353-356: 213-216.